

Justyna Zygmuntowicz<sup>1,\*</sup>, Joanna Tańska<sup>2</sup>, Paulina Wiecińska<sup>2</sup>, Paulina Piotrkiewicz<sup>1</sup>, Katarzyna Konopka<sup>1</sup>, Mikołaj Szafran<sup>2</sup>, Marcin Wachowski<sup>3</sup>, Bartosz Michalski<sup>1</sup>, Waldemar Kaszuwara<sup>1</sup>

<sup>1</sup>Warsaw University of Technology, Faculty of Materials Science and Engineering, 141 Woloska St., 02-507 Warsaw, Poland

<sup>2</sup>Warsaw University of Technology, Faculty of Chemistry, 3 Noakowskiego St., 00-664 Warsaw, Poland

<sup>3</sup>Military University of Technology, Faculty of Mechanical Engineering, 2 gen. S. Kaliskiego St., 00-908 Warsaw, Poland

\* Correspondence: justyna.zygmuntowicz@pw.edu.pl

Received (Otrzymano) 28.05.2025

## Gradient Al<sub>2</sub>O<sub>3</sub>-Ni composites for aggressive substance transport: a novel approach using centrifugal gel casting

<https://doi.org/10.62753/ctp.2025.09.2.2>

This study focuses on the development and characterization of Al<sub>2</sub>O<sub>3</sub>-Ni composite materials designed for use in environments where high corrosion resistance and mechanical strength are critical. The composites were formed using the centrifugal gel casting method to produce pipes with a gradient structure. The inner layer of the pipes consisted mainly of Al<sub>2</sub>O<sub>3</sub>, while the outer layer incorporated nickel particles. Rheological, thermogravimetric, and microstructural analyses were conducted to optimize the composite's formulation and processing conditions. The results showed that a monomer content of 3% by weight of 2-hydroxyethyl acrylate (HEA) provided an optimal balance between workability and polymer network formation. Corrosion tests revealed that while the alumina-rich inner layer exhibited good chemical resistance, the presence of nickel particles on the surface led to localized corrosion, particularly in acidic environments. The findings indicate that further refinement of the casting process is necessary to improve the distribution of the nickel particles and enhance the material's overall corrosion resistance.

**Keywords:** HEA, composites, Al<sub>2</sub>O<sub>3</sub>-Ni, gel casting, FGM

### INTRODUCTION

An oxide material of special ceramics resistant to many aggressive substances used in the chemical industry is Al<sub>2</sub>O<sub>3</sub> [1]. This material is characterized by chemical inertness [2–3]. It has high creep resistance [3]. Currently available technological processes allow pipes to be formed from this material [4]. Alumina is relatively inexpensive compared to other special ceramic materials. At the same time, products made of Al<sub>2</sub>O<sub>3</sub> provide high abrasion resistance due to their high hardness [5]. However, during the forming of corundum elements, problems related to resistance to the brittle fracture of ceramics may occur. The answer to this problem may be composites from the ceramic-metal system [6]. Moreover, the optimal material

for this type of application may be gradient composites, where the inner layer of the pipe would contain only Al<sub>2</sub>O<sub>3</sub> ceramics, while the surface (outer) layer would contain metallic particles, e.g. nickel, distributed in a ceramic matrix [7]. The share of metallic particles should decrease gradually (gradient) towards the pipe axis [8]. This type of structure provides increased resistance to cracking in the surface layer because metallic particles prevent crack migration [7–9]. The gradient nature of the structure means that the material's own stresses, resulting from, for example, the different thermal expansion of both components, will change continuously [7–9].

In connection with this work, an attempt will be made to determine the optimal structure of the material, which will be made taking into account the working conditions of the element, based on available literature knowledge and the experience of the team. The essence of the study will be to develop a technological process that will ensure the optimal microstructure of pipes for transporting aggressive substances at elevated temperatures is obtained. Therefore, simulation-based corrosion tests will be conducted in artificial corrosive environments. These tests are a reliable and fast way to assess the destructive effects of the environment on the manufactured elements. The results of corrosion tests will allow us to predict the rate of destruction of pipe elements in the conditions of their actual use. In the first stage of the research, the work will focus on the selection of appropriate components of gelling masses, especially the monomer, from among commercially available substances. Most often in the gel casting method, monomers from the acrylate group are used [9–10]. Therefore, in this experiment, work will be carried out using the 2-hydroxyethyl acrylate methacrylamide (HEA) monomer [11]. The development of a precise recipe for obtaining the pipe-shaped specimens was a key step in ensuring the repeatability and structural integrity of the composite. The next stage will be to determine the microstructural properties. This task is a continuation and development of the work started in the first part of the experiment concerning selection of the appropriate components of the casting slips. This work will begin with rheological and thermogravimetric tests. Then, microstructural observations will be performed. One of the basic elements of the quality assessment of the obtained samples will be the assessment of their surface condition and microstructure. Microstructural tests will be carried out by means of scanning electron microscopy on fragments cut from samples obtained in the centrifugal gel casting process. Stereological methods will be employed for quantitative characterization of the microstructure of the produced composites. The use of stereological tests will allow the average size of metallic particles in the

specimens to be determined, as well as the effect of the Ni content on the growth of Al<sub>2</sub>O<sub>3</sub> grains during the sintering process. The stereological parameters will be determined using the MicroMeter v.086b program based on microscopic observations [12–14]. Together with other tests, they will enable the type and characteristics of the microstructure of the manufactured pipes to be ascertained. Depending on the adopted casting parameters, the aim will be to obtain a gradient material. A gradient change in the structure would eliminate abrupt changes in thermal stresses. A structure with an increased share of the metallic phase in the surface layer should additionally enable easy use of soldering. In addition, the apparent density, relative density and water absorption will be determined by the hydrostatic method. What is more, the tests will include analysis of the chemical composition. The most common causes of damage to the structure include corrosive processes. These processes occur in particular where we deal with welded joints, i.e. in industrial installations and communication infrastructure. Therefore, it is very important to perform corrosion tests of the manufactured elements in the next stage of the research. Corrosion tests will allow a quick, comparative assessment of the resistance of pipe samples in the tested media. In addition, they will enable the degree of aggressiveness of the acidic or alkaline environment on the tested element to be determined. In addition, they will allow the suitability of the pipes proposed in the experiment to be ascertained for structural applications, machines or installations. It should be emphasized that a significant novelty in the proposed experiment is the possibility of adapting the proposed method of forming elements with a diverse chemical composition to transport aggressive substances such as inorganic acids and bases.

## MATERIALS AND METHOD

Commercially available powders, nanometric Al<sub>2</sub>O<sub>3</sub> (TM-DAR) and micrometric Ni (Sigma Aldrich) were used as the starting materials in the process. Demineralized water was utilized as the

solvent, 2-hydroxyethyl acrylate (HEA) as the monomer, and N,N,N',N'-tetramethylethylenediamine TEMED (1 wt% relative to the monomer mass) was employed as the activator. The polymerization reaction initiator was ammonium persulfate (APS) (2 wt% relative to the monomer mass). Diammonium hydrogen citrate (DAC) was used as a liquefier in the amount of 0.3% by weight.

### Idle time measurements

One of the key parameters in the centrifugal gel casting process is determining the idle time, i.e. the time from adding the initiator and activator to the system to the macroscopically observable increase in viscosity resulting from the polymerization reaction. For this purpose, it is very important to select the appropriate amount and type of initiator as well as activator for the tested system. This is evidenced by the research conducted by Kokabie et al. [15]. They showed in their work that the gelation process of a colloidal system based on alumina with the addition of acrylamide and acrylic acid is most influenced by the content of the initiator [15]. Literature data indicate that it is most beneficial for the idle time to be between 4 minutes and 1 hour [16-17]. Determining the idle time is a very important parameter from the point of view of the employed technology. A too long idle time extends the process of forming the samples, which consequently adversely affects the economic aspects of the entire production process. Nevertheless, a too short idle time may be insufficient to cast the slip in the mold in which the casting process is to take place. Therefore, in the first stage of the study, it was proposed to conduct an experiment that would allow the idle time to be determined for the casting slip based on HEA. For this purpose, casting slips were prepared with a solid phase content of 50% by volume (of which 90% was  $\text{Al}_2\text{O}_3$ , and 10% – Ni). The masses differed in the content of monomer (2-hydroxyethyl acrylate HEA) – 1 wt%, 3 wt%, 5 wt% or 7 wt% in relation to the total mass of powders. The liquefying agent was diammonium hydrocitrate

(0.3 wt% of the total powder mass), water was the solvent, and N,N,N',N'-tetramethylethylenediamine TEMED (1 wt% relative to the monomer mass) was used as the activator. The masses were mixed in a Retsch PM200 mill for 1 h at the speed of 300 rpm, and then ammonium persulfate APS (2 wt% relative to the monomer mass) was added. The last stage of mass preparation was their mixing and deaeration in a Thinky ARE-250 device for 1 min at the speed of 2,000 rpm. For the casting slips prepared in this way, measurements of the idle time were determined, which were performed on a Brookfield RVDV – II + PRO viscometer using a 34 spindle. The spindle speed was 3.5 rpm. The measurements were carried out until the moment when the viscosity increased intensively, which indicates the actual initiation of the polymerization reaction in the casting slip and the formation of polymer chains. All the rheological tests were carried out at room temperature.

Based on the studies conducted to determine the idle time, one casting slip characterized by the optimal idle time was selected for further studies. Further experiments were carried out utilizing this mass, including determination of the rheological properties, i.e. the dependence of viscosity on the shear rate, dependence of shear stress on the shear rate and the dependence of elastic modulus ( $G'$ ) and viscous modulus ( $G''$ ) on deformation at a constant frequency. Then, thermogravimetric tests were carried out. Composites were produced for which selected physical parameters were determined, macroscopic and microscopic observations were carried out, EDS analysis and stereological analysis were performed to determine the content of the metallic phase in individual zones.

### Rheological tests

Rheological measurements were performed for the casting slip with a solid phase content of 50 vol.% (of which 90% was  $\text{Al}_2\text{O}_3$  and 10% – Ni), characterized by a monomer content (HEA) of 3 wt% in relation to the sum of powder masses. The liquefying agent was diammonium hydrocitrate (0.3 wt% of the total powder mass), water

was used as the solvent, and TEMED (1 wt% of the monomer mass) was used as the activator. The masses were mixed in the Retsch PM200 mill (1 h; 300 rpm).

### Thermogravimetric studies

Thermal analysis involves examining the physical and chemical changes that occur as a sample is heated [18]. This category of analysis includes methods such as thermogravimetric analysis (TG) and differential thermal analysis (DTA) [18]. TG measures the mass loss associated with each transformation or reaction during heating, and when combined with differential thermal effects, it enables both quantitative and qualitative interpretation of the sample composition [19]. Additionally, thermal analysis allows the temperature range and peak temperatures to be determined at which these transformations or reactions occur.

During thermal analysis, a thermogravimetric (TG) curve is recorded, showing the mass change of the sample as a function of temperature, along with the differential thermal analysis (DTA) curve, which depicts the endothermic and exothermic processes during heating [19-20]. The measurement process involves recording the temperature difference between the sample and a reference material. A derivative thermogravimetric (DTG) curve is also generated, which helps in identifying the start and end temperatures of each transformation or reaction.

Thermogravimetric analysis in this study was conducted using a Netzsch STA 449C device coupled with a Netzsch QMS 403C mass spectrometer. The analysis was performed on a casting slip with a solid phase content of 50 vol.% by volume, consisting of 90% Al<sub>2</sub>O<sub>3</sub> and 10% Ni. DAC was used as the fluidizer at 0.3 wt%, HEA as the monomer at 3 wt%, TEMED as the activator at 1 wt%, and APS as the reaction initiator at 2 wt%. The quantities of monomer and fluidizer were calculated based on the total mass of the powders, while the activator and initiator quantities were based on the organic monomer mass. TEMED was used as a 10% aqueous solution, and APS as a 5% aqueous solution. Measurements for samples containing

metal powder were conducted in an argon atmosphere.

The analysis involved placing a reference crucible containing alumina calcined at 1500°C and a measuring crucible containing the sample, weighed with an accuracy of 0.0001 g, into a furnace. The sample was subjected to a controlled temperature program: from 25°C to 600°C at the rate of 1°C/min, from 600°C to 1400°C at 2°C/min, followed by holding at 1400°C for 2 hours.

### Forming method

Obtaining Al<sub>2</sub>O<sub>3</sub>-Ni composites in the form of pipes with a gradient structure is ensured by the method of gel centrifugal slip casting [7]. This method combines traditional slip casting into molds with a radical polymerization reaction. An aqueous solution of a reactive organic monomer, activator, water and dispersion agents (i.e. liquefiers) are added to the powder mixture (alumina + nickel). The suspension prepared in this way is subjected to homogenization. In the next step, a free radical initiator is added to the suspension to accelerate the polymerization reaction. The process of polymerization of the organic monomer in the casting slip begins under the influence of the initiator added to the mass. The measure of the optimal amount of initiator is the time after which a rapid increase in mass viscosity is observed. The amount of initiator added allows process control, which in consequence ensures the proper course of the process of shaping the finished product. Then the obtained casting slip is poured into the mold. The process of centrifugal slip casting with simultaneous free-radical polymerization reaction is carried out. After gelation, the formed product is removed from the mold, dried and then sintered. The sintering process was carried out in a Nabertherm RHTC 80-230/16 pipe furnace. The samples to be sintered were placed in a ceramic mold on a coarse-grained corundum backfill. The mold with the samples was placed in the heating zone of the furnace horizontally along the length of the sintering chamber. The samples were placed on the corundum backfill so that they did not touch

each other or the side edges of the mold. The sintering process was experimentally determined based on thermogravimetric studies and previous experimental work. The sintering process was divided into four stages. Heating the furnace to reach the sintering temperature was divided into two stages differentiated by the rate of temperature increase. In Stage I, from room temperature to 600°C, the furnace was heated at the rate of 1°C/min, after reaching 600°C, the heating rate was increased to 2°C/min until the maximum temperature was reached, i.e. the sintering temperature of 1400°C. The sintering process at 1400°C was carried out for 2h. Then the samples were subjected to controlled cooling at the rate of 2°C/min until room temperature was reached. The use of a reduced temperature increase rate in Stage I was directly related to the presence of organic substances in the prepared samples, which undergo thermal decomposition in the temperature range of Stage I. Reducing the rate of temperature increase provides greater control over the course of this process. Additionally, slow heating to the maximum temperature and cooling (2°C/min) were employed to limit the temperature gradient over time, as well as to possibly minimize the formation of defects in the sintered materials due to the temperature gradient and stresses occurring in the material, among others owing to the large variation in the thermal expansion coefficients of the components. The sintering temperature of the produced materials was lower than the adopted sintering temperature range for corundum ceramics, related to the use of Al<sub>2</sub>O<sub>3</sub> powder with a nanometric grain size in the matrix, which, according to previous studies, is densified at lower temperatures. In addition, the process required a lower temperature than the standard one, resulting from the melting temperature of nickel, which is 1455°C. In order to carry out the process taking place entirely in the solid phase of the components, it was necessary to use a sintering temperature lower than the melting temperature of the metallic phase included in the composite.

The condition for obtaining a material free of structural defects is proper selection of the casting slip and the parameters of the casting and sintering process.

## Physical properties test

Selected physical properties of the sintered samples were ascertained by means of the Archimedes method (PN-76/E-06307 standard). The measurements were taken at room temperature, hence the density of the water used for the calculations was 0.997 g/cm<sup>3</sup>. The relative density was determined by comparing the apparent density obtained from the measurement with the theoretical density of the sintered sample. The theoretical density was determined from the rule of mixtures and it was 4.48 g/cm<sup>3</sup>.

## Microscopic observations

Microstructural analysis of the ceramic-metal composites was done utilizing scanning electron microscopy (SEM). The composite samples were prepared using metallographic techniques for detailed observation. Cross-sections of the sintered composite samples cut into 1 cm fragments from the middle were embedded in conductive resin and then ground and polished. The microscopic observations were conducted with a JEOL JSM-6610 SEM at 15 kV, providing high-resolution imaging of the material microstructure. This preparation enabled accurate and reproducible analysis, which is essential for understanding the microstructure of the composites. Additionally, in order to evaluate the composites after corrosion tests, observations were carried out by means of a Keynes microscope. The employed microscope allows the observation of uneven surfaces and three-dimensional objects with a clear image, obtained thanks to the large depth of focus and large observation distance.

## Image analysis

This study quantitatively analyzes the metallic phase content using image analysis techniques. Micrographs of randomly selected composite areas, each containing at least 2000 metallic phase particles, were analyzed with MicroMeter software [12–14]. Multi-tone micrographs were binarized to isolate and measure the metallic phase and alumina grain sizes. The analysis provided data on the size distribution of the metallic particles.

## Corrosion tests

The corrosion resistance testing of the Al<sub>2</sub>O<sub>3</sub>-Ni composite specimens followed the methodology described by J. Travaglini et al. [21]. The corrosion resistance was assessed utilizing an immersion method in both alkaline and acidic solutions. In this method, the samples are submerged in corrosive solutions with specific pH and concentration, and observations are made regarding changes in the material structure, mass, as well as dimensions during and after exposure. These observations are conducted at predetermined intervals.

According to the PN-76/H-04602 standard, corrosion tests are performed on specially prepared specimens in natural liquids, industrial solutions, or laboratory-prepared solutions, either at room temperature or at a constant elevated temperature. The specimens must be fully immersed in the solution, with a recommended liquid-to-specimen surface area ratio of 10:1. The total testing duration is determined based on the corrosion rate.

In this study, the specimens were immersed in a 7.6% HCl acid solution and a 0.1 g/l NaOH alkaline solution. The observations focused on two surfaces: the inner surface, primarily composed of ceramics, and the cross-section, to monitor changes in both the internal structure and the corrosion resistance gradient across the metal-ceramic interface. The specimens were cut using a precision saw and metallographic sections were prepared with #600 and #1200 grit papers for microscopic examination. Initially, the specimens were weighed and subjected to macroscopic and microscopic analyses employing a metallographic microscope and a scanning electron microscope.

The prepared specimens were then immersed in the HCl and NaOH solutions. Observations after exposure to the corrosive environment were conducted at seven-day intervals over four weeks. After each interval, the specimens were removed from the solution, cleaned with acetone to eliminate any residue, weighed, and re-examined by means of both macroscopic and microscopic techniques. Figure 1 shows the specimens intended for corrosion tests after cutting and preparation in their initial state. As can be seen, the specimens

are free of surface defects and cracks that could disrupt the mechanism of a possible corrosion process.

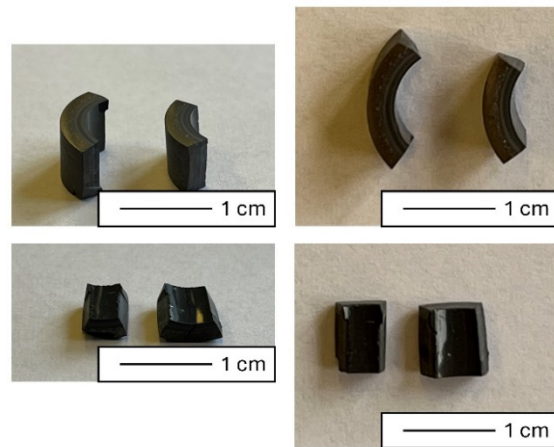


Fig. 1. Al<sub>2</sub>O<sub>3</sub>-Ni specimens prepared for corrosion tests

The prepared specimens in their initial state were also subjected to observations by a metallographic microscope. The results are presented in Figure 2. The observations confirmed the absence of cracks in the structure of the prepared specimens. Considering the fact that nickel is a component definitely susceptible to corrosion, in the case of surface observation, the appearance of corrosion centers is expected precisely in the zone rich in metal. In the case of Al<sub>2</sub>O<sub>3</sub> ceramics, a component with high corrosion resistance and resistance to aggressive environments, corrosion resistance to both acid and alkaline solutions is expected. Nonetheless, it is worth noting that the samples are characterized by a gradient structure in the cross-section, which may affect the inhomogeneous course of the entire process, and that the presence of a small amount of metallic inclusions is visible at the surface of the inner zone, which may result in reduced corrosion resistance of the ceramics (the creation of corrosion centers in the place of the component with lower resistance).

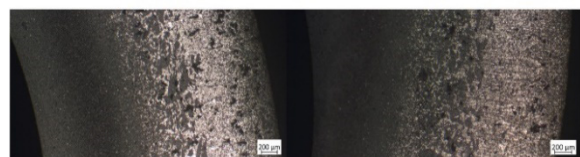


Fig. 2. Cross-sections of cut specimens of Al<sub>2</sub>O<sub>3</sub>-Ni sample intended for corrosion tests

## RESULTS AND DISCUSSION

The results of the idle time measurements for the masses with 1 wt% and 3 wt% HEA content are presented in Figure 3. In the case of masses with the monomer content of 5 wt% and 7 wt%, measurements could not be performed because both masses gelled immediately after adding the initiator (during mixing in the Thinky device). For the mass containing 3 wt% HEA, the idle time is about 8 minutes. This is the time that enables good distribution of the initiator and homogenization of the suspension, and then casting it into molds. For the mass containing 1 wt% HEA, no increase in viscosity was observed, which means that the mass did not gel. This was most likely caused by too little monomer in the suspension, which prevented the formation of polymer chains.

Studies have shown that the optimum monomer content is 3 wt%. The addition of 1 wt% HEA is insufficient to create a polymer network in the casting slip that immobilizes ceramic powder particles, while the addition of 5 wt% and 7 wt% results in a too short idle time. Based on the studies conducted to determine the idle time, the casting slip containing 3 wt% monomer was selected for further studies.

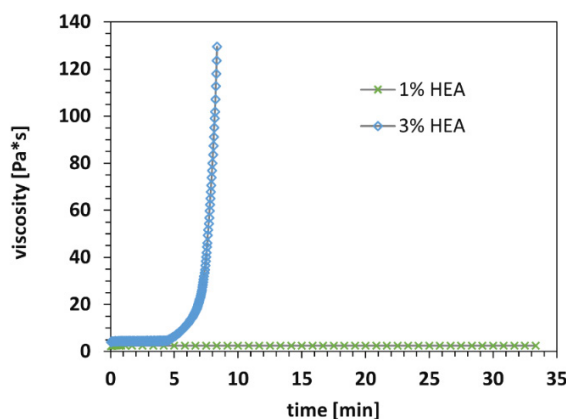


Fig. 3. Dependence of viscosity on time for masses with the addition of 1 wt% and 3 wt% HEA

The next step was to focus on rheological tests for the mass containing 3 wt% monomer. Figure 4 shows the dependence of viscosity on the shear rate (the so-called viscosity curve) for the suspension containing 3 wt% HEA. Based on the graph,

it can be concluded that the tested suspension belongs to non-Newtonian fluids thinned by shear, because with increasing shear rate, a decrease in its viscosity is observed. The measurements showed that the viscosity of the suspension at 1 s<sup>-1</sup> [Pa\*s] with increasing shear rate was 4.67 [Pa]. On the other hand, the viscosity at 1 s<sup>-1</sup> [Pa\*s] with decreasing shear rate was 4.96 [Pa].

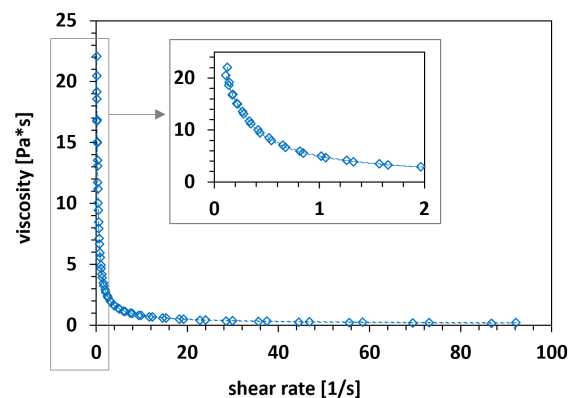


Fig. 4. Dependence of viscosity on shear rate

Then the dependence of shear stress on the shear rate, i.e. the so-called flow curve for the tested suspension, was determined, the obtained results of which are presented in Figure 5. The graph clearly shows the so-called hysteresis loop, which indicates that this is a rheologically unstable, thixotropic fluid. Based on the graph presented in Figure 4, it was found that the tested casting slip is characterized by a flow limit of 2.73 [Pa].

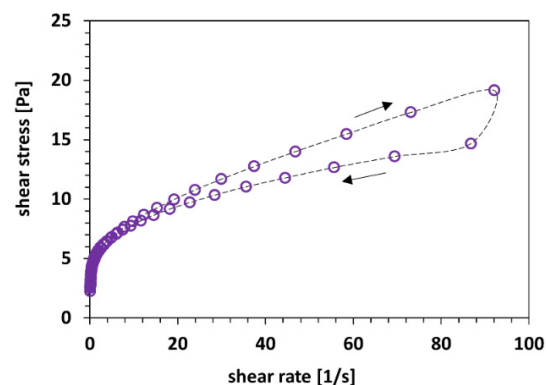


Fig. 5. Dependence of shear stress on shear rate (flow curves)

Based on the measurements of the elastic ( $G'$ ) and viscous ( $G''$ ) moduli at variable deformation,



the range of deformation values was determined at which  $G'$  and  $G''$  do not change, the so-called linear viscoelasticity range (LVER). The graphs illustrating the LVER measurement results are presented in Figure 6. In the next step, the deformation value (0.02%) was selected from the LVER. At the given deformation, the dependence of the  $G'$  and  $G''$  moduli on the frequency was then determined (Figure 6). The obtained curves are consistent with the expectations and indicate that elastic features dominate over viscous ones in the tested suspension.

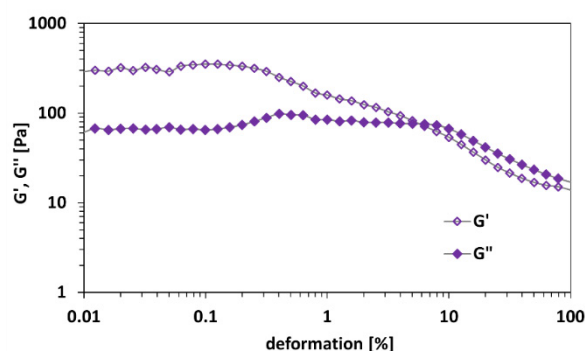


Fig. 6. Dependence of elastic modulus ( $G'$ ) and viscous modulus ( $G''$ ) on deformation at constant frequency

The results of this study demonstrate the potential of the Al<sub>2</sub>O<sub>3</sub>-Ni composites for use in chemically aggressive environments but also highlight areas where the material performance could be improved. The use of the 3 wt% HEA monomer was found to be optimal for achieving a balance between the necessary workability of the casting slip and the formation of a stable polymer network capable of immobilizing ceramic particles. This finding is critical for ensuring that the material can be reliably produced on an industrial scale.

The rheological properties of the casting slip were characterized by non-Newtonian behavior, which is typical for suspensions with a high solid content. The thixotropic nature of the slip, as indicated by the hysteresis loop in the flow curve, suggests that the material is well-suited for processes where shear thinning is advantageous, such as in centrifugal casting. Nevertheless, the flow limit observed at 2.73 Pa highlights the need for careful control of the shear conditions during processing to avoid defects.

Figure 7 displays the results of thermal analysis for the 3 wt% HEA mass. Based on the DTA, TG and DTG curves, it can be concluded that the total mass loss is 15.91% and is related to the loss of water and decomposition of organic compounds. The DTA curve shows two endothermic peaks – at temperatures of approx. 55°C and approx. 103°C, which are related to the dehydration process – the removal of -OH groups. This is also confirmed by signals from the mass spectrometer ( $m/z$  17 and  $m/z$  18). The decomposition of the organic phase is observed in the temperature ranges of 200°C–500°C and 1000°C–1350°C. In these temperature ranges, signals are observed that can be attributed to the release of CO<sub>2</sub> from the sample. The  $m/z$  32 signal indicates the release of small amounts of oxygen from the sample.

The value of the mass loss resulting from the decomposition of organic substances does not exactly match the amount of additives used during the preparation of the casting masses. The error may result from the fact that the specimens taken for analysis are small (approx. 0.2–0.3 g), owing to the small capacity of the measuring crucible. A small amount of individual additives is distributed in several dozen milliliters of suspension, thus the sample fragment that was analyzed may contain less than their assumed amounts.

Similar thermogravimetric measurements regarding sample formation were performed in previous work by CGC [7]. Nonetheless, the previous experiment focused on the thermal analysis of a pure polymer derived from glycerol monoacrylate [7]. Earlier work described the decomposition behaviour and the mass loss stages of this polymer when measured in air [7]. Moreover, it emphasized a detailed breakdown of the polymer's thermal degradation, identifying specific degradation steps, temperatures, and corresponding  $m/z$  values [7]. In this research, it was decided to analyze the 3 wt% HEA mass within a composite material. The obtained results provided details about the dehydration and decomposition stages, particularly concerning water and organic compounds. This study concentrated more on the initial dehydration and later decomposition of the organic phase, with



broader temperature ranges and potential errors in the mass analysis. The research conducted in this article discussed a composite  $\text{Al}_2\text{O}_3$ -Ni sample with a focus on water removal and organic decomposition, highlighting issues with accuracy due to the experimental setup. The thermal events occur over broader and higher temperature ranges in comparison to the previous study and with more emphasis on endothermic dehydration [7].

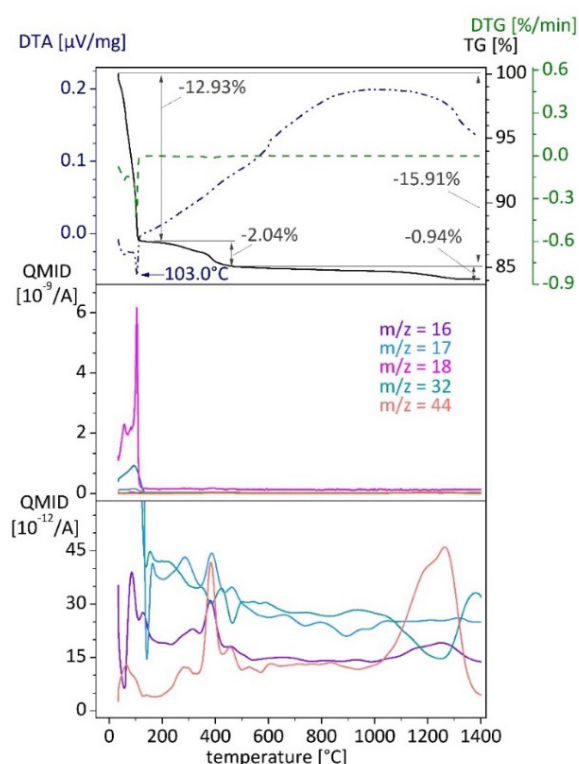


Fig. 7. Thermal analysis results for 3 wt% HEA mass: a) TG, DTG, DTA curves; b) change in intensity of m/z values as a function of temperature; c) enlargement of fragment from graph b).

The thermogravimetric analysis provided insights into the decomposition behavior of the composite material, particularly the loss of water and organic compounds. The presence of endothermic peaks corresponding to the removal of hydroxyl groups and the decomposition of the organic phase suggests that the material undergoes significant physical and chemical changes during sintering.

During the sintering process, it was possible to obtain sinters with good density, free from surface defects and cracks. This leads to the conclusion that the applied sintering process stages, together

with the specified parameters of their execution, were selected in a way that ensured satisfactory sinters were obtained. Example photos showing the pipes obtained by centrifugal gel casting are presented in Figure 8. The produced samples were characterized by a relative density of  $96.55 \pm 1.23\%$ , open porosity of  $5.57 \pm 1.96\%$  and water absorption of  $1.29 \pm 0.47\%$ .

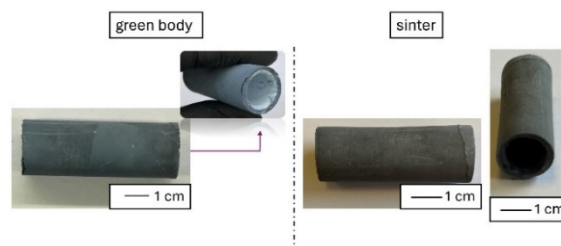


Figure 8. Samples produced by CGC method before and after sintering process.

Microscopic observations confirmed the gradient distribution of the metallic phase on the cross-section of the obtained samples. An example of an SEM micrograph showing the cross-section of an  $\text{Al}_2\text{O}_3$ -Ni sample formed by the CGC method is presented in Figure 9. It was conventionally assumed that the produced pipes are characterized by a three-zone structure. Each zone is characterized by a different share of the metallic phase. The nickel content decreased with the distance from the outer edge of the sample. The image analysis showed that Zone I was characterized by a 34% volume share of the metallic phase, while Zone II was characterized by a 17% volume share of the metallic phase, while in Zone III the content of the metallic phase was equal to  $>1\%$ .

A similar microstructure was obtained in previous studies on sample formation by the CGC method, however, using a different monomer in the form of glycerol monoacrylate (GM) [7].

Image analysis revealed that the average particle size of the metallic phase in Zone I was  $3.91 \pm 0.41 \mu\text{m}$ , while in Zone II it was  $3.26 \pm 0.87 \mu\text{m}$ , and in Zone III  $2.23 \pm 0.22 \mu\text{m}$ . Based on the obtained results, it was found that with the distance from the outer edge of the sample to its interior, the average nickel particle size decreases.

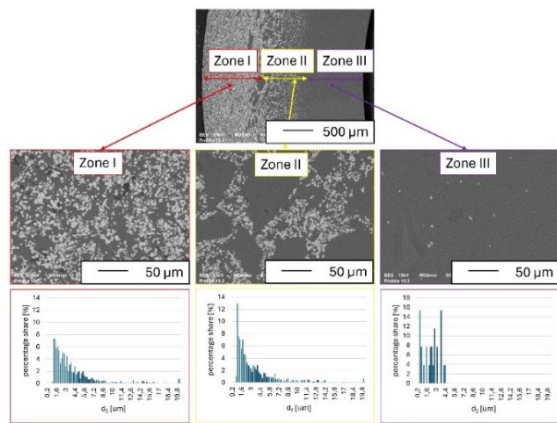


Fig. 9. Example cross-section of  $\text{Al}_2\text{O}_3$ -Ni sample formed by CGC method, with histograms showing metallic phase distribution in individual zones

Analysis of the chemical composition showed that the composite contains three components: aluminum, oxygen, nickel. The obtained results are given in Figure 10.

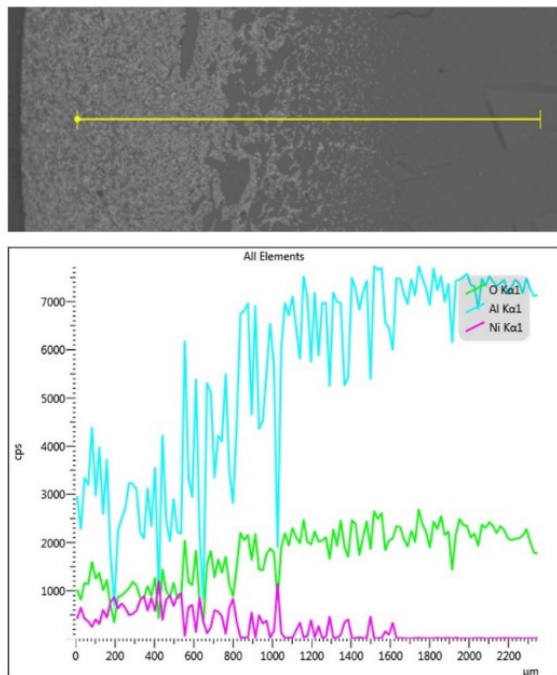


Fig. 10. Linear EDS results showing distribution of elements in composite

The next step was to focus on the corrosion tests. Detailed observations of the specimens were carried out during the experiment, the results of which are presented in Figures 11–13. Two specimens cut out of the samples were subjected to corrosion tests. In the further part of the tests they will

be called respectively the large and small specimen (Figure 11). Moreover, from the point of view of applying the obtained  $\text{Al}_2\text{O}_3$ -Ni composite, the most important are corrosion tests of the inner surface of the pipe. This is the surface potentially exposed to contact with aggressive substances. Micrographs of this surface after the specimen was exposed to selected environments are presented in Figure 12.

The tests in an acidic environment showed that in the case of both specimens, a change in mass was observed compared to the initial state. It was found that the mass of the small specimen in the acidic environment decreased by 15.49% after 1 week, by 21.60% after 2 weeks, by 23.06% after 3 weeks, and by 22.74% after 4 weeks compared to the initial mass. In the case of the larger specimen, it was observed that after 1 week the sample decreased by 13.57%, after 2 weeks by 20.97%, after 3 weeks by 22.52%, and after 4 weeks by 22.57% compared to the initial mass. Interestingly, in the case of the alkaline environment, a slight increase in the mass of the specimens was observed over 4 weeks. In the case of the small specimen, after 1 week, a 0.35% increase in mass was observed, while after 2 weeks, the mass increased by 0.61%, and after 3 weeks, there was a 0.52% increase in mass, and after 4 weeks, 0.46% in relation to the initial mass. In the case of the larger specimen tested in the alkaline environment, a slight increase in mass was also observed. After 1 week, the specimen changed its mass by 0.60%, and after 2 weeks, the mass increased by 0.81%, while after 3 weeks it was 0.80%, and after 4 weeks, the specimen mass increased by 0.64% in relation to the initial mass.

The obtained mass loss values for the specimens after exposure to acidic medium were confirmed by the SEM observations (Figure 13). On the observed surfaces (Figure 13 a)) after 1 week, corrosion spots appear, visible as surface defects. It should be assumed that they are in places where nickel particles occur. When planning the described tests, it was assumed that centrifugal casting would cause all the nickel particles to move towards the outer surface, and the zone at the inner

surface would consist only of  $\text{Al}_2\text{O}_3$ . This would provide it with excellent chemical resistance. The obtained results indicate that this assumption was incorrect and that single particles or clusters of nickel particles occur on the inner surface of the specimen. This was confirmed by stereological analysis, which showed that Zone III in the specimens are characterized by a small amount of nickel (Figure 9).

The presence of nickel particles on the internal surface can be caused by two phenomena. The first one results from the action of nickel as a catalyst of the polymerization reaction. It is possible that even before the mass is introduced into the mold and the centrifuge is started, large areas (envelopes) of polymer develop around some nickel particles. This can cause such an agglomerate to have a lower total density. At the same time, starting the centrifuge causes a hole to form inside the mold, i.e. a new surface is created between the casting mass and the air. This surface is characterized by a certain level of surface tension, which can hold solid particles, acting effectively against the centrifugal force. This can be particularly effective when the surface of the metal particle is increased by the polymerizing monomer. It should therefore be stated that the tested technology does not provide complete internal chemical resistance (inertness). The studies also show that the number of corrosion defects does not increase with long exposure. Only nickel particles located on the surface are dissolved, while others are protected under the  $\text{Al}_2\text{O}_3$  layer. Unfortunately, this phenomenon negatively affects the smoothness of the inner surface of the pipe.

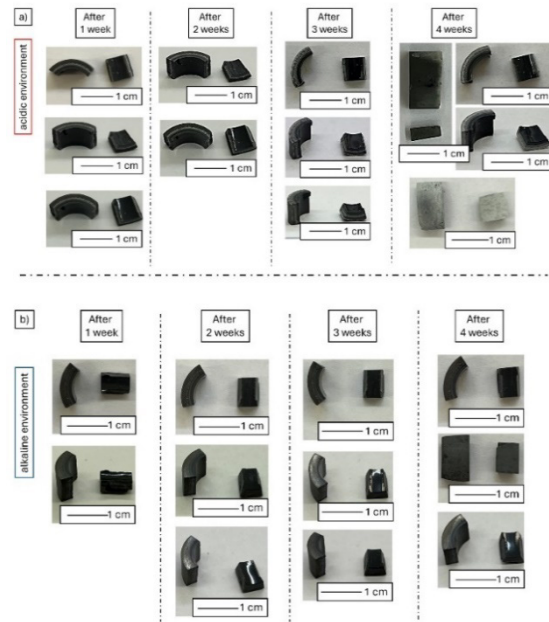


Fig. 11. Photos of specimens after four weeks of exposure to (a) acidic environment and (b) alkaline environment

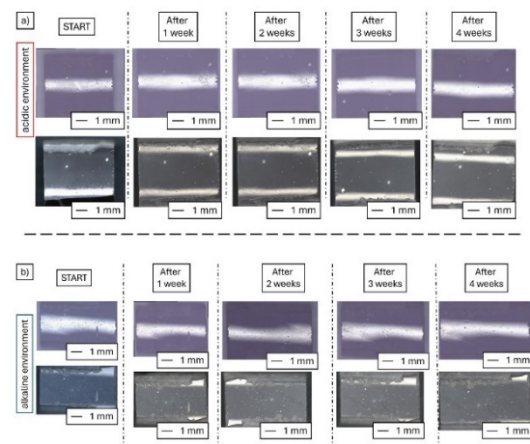


Fig. 12. Micrographs of specimens after four weeks of exposure to (a) acidic environment and (b) alkaline environment showing external and internal surfaces – Keynes microscope



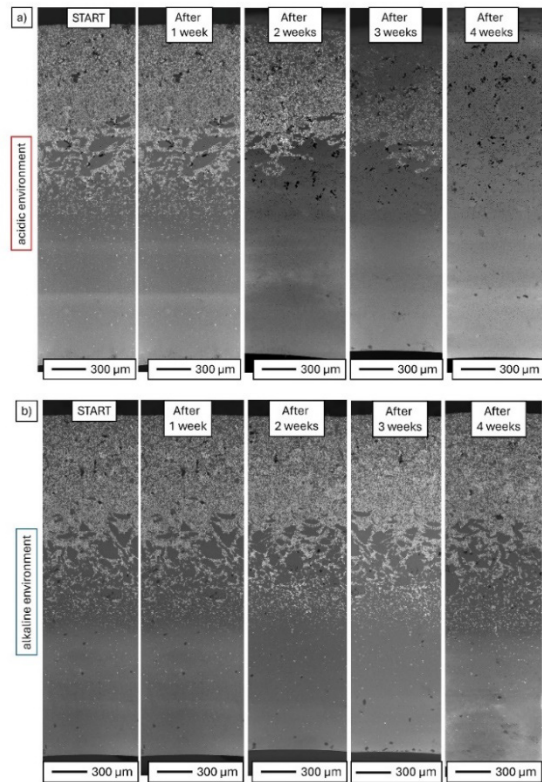


Fig. 13. Microstructure of specimens at 0-4 weeks of exposure to (a) acidic environment and (b) alkaline environment – SEM

The corrosion tests revealed that while the Al<sub>2</sub>O<sub>3</sub> component provided good resistance to both acidic and alkaline environments, the nickel particles on the inner surface significantly compromised this resistance. The observed mass loss in acidic conditions, coupled with the appearance of surface defects visible in the SEM micrographs, underscores the need for further process optimization to prevent the nickel particles from migrating to the inner surface during casting.

## CONCLUSIONS

The article investigates the development of Al<sub>2</sub>O<sub>3</sub>-Ni (alumina-nickel) composite materials designed for use in chemically aggressive environments, particularly in industries that require high resistance to corrosion and mechanical wear. The study focuses on creating pipes with a gradient structure, where the outer layer is predominantly alumina for chemical inertness, while the inner layer contains nickel particles.

The study used commercially available nanometric Al<sub>2</sub>O<sub>3</sub> and micrometric Ni powders. The centrifugal gel casting method was employed to form the composite pipes, combining slip casting with free-radical polymerization to ensure a gradient distribution of the nickel particles.

Rheological tests identified that a 3% by weight content of 2-hydroxyethyl acrylate (HEA) monomer provided an optimal balance between workability and the creation of a stable polymer network in the green body samples. Thermogravimetric analysis revealed the decomposition stages of organic components and the removal of water, providing insight into the thermal stability of the composite.

Scanning electron microscopy confirmed the gradient distribution of the nickel phase within the composite, with a higher concentration near the surface and a decrease towards the core. This structure aims to enhance the material's mechanical integrity while maintaining chemical resistance.

The composite's resistance to acidic (HCl) and alkaline (NaOH) environments was assessed. While the alumina-rich inner layer showed good resistance, the presence of nickel particles on the surface led to localized corrosion, especially in acidic conditions. The study found that corrosion did not progress significantly with time, suggesting that only the nickel particles exposed at the surface were affected.

The research demonstrated that while the Al<sub>2</sub>O<sub>3</sub>-Ni composite shows promise for applications requiring a combination of mechanical strength and chemical resistance, improvements are needed to prevent the nickel particles from reaching the inner surface where they could compromise corrosion resistance. Future work should focus on refining the casting process to enhance the distribution and incorporation of nickel particles within the alumina matrix. Specifically, strategies to better control the distribution of the nickel particles and ensure their complete segregation to the outer layer should be explored. This could involve adjustments to the centrifugal casting

parameters or the introduction of additional steps to remove or isolate the nickel particles from the inner surface of the pipes.

This study provides a foundation for developing advanced materials for use in harsh chemical environments, with potential applications in the chemical, petrochemical, and related industries.

### Declaration of competing interests

The authors declare that they have no known competing financial interests or personal relationships that could have appeared to influence those works reported in this paper.

### Acknowledgments

This publication was supported by grant No. TANGO-V-A/0004/2021 from the National Centre for Research and Development.

### REFERENCES

- [1] Shanaghi A., Chu P.K., Souri A.R., Mehrjou B., Advanced Ceramics (Self-healing Ceramic Coatings). [In:] Ikhmayies, S.J. (eds) Advanced Ceramics. Advances in Material Research and Technology. Springer, Cham. 2024, [https://doi.org/10.1007/978-3-031-43918-6\\_4](https://doi.org/10.1007/978-3-031-43918-6_4).
- [2] Xu H., Li S., Liu R. et al., Fabrication of alumina ceramics with high flexural strength using stereolithography. *Int J Adv Manuf Technol* 2023;128:2983–2994, <https://doi.org/10.1007/s00170-023-12100-x>.
- [3] Abyzov A.M., Aluminum Oxide and Alumina Ceramics (review). Part 1. Properties of  $\text{Al}_2\text{O}_3$  and Commercial Production of Dispersed  $\text{Al}_2\text{O}_3$ . *Refract Ind Ceram* 2019;60:24–32, <https://doi.org/10.1007/s11148-019-00304-2>.
- [4] Doremus R.H., Alumina-silica system, Handbook of ceramics and composites. Vol. 1: Synthesis and properties; ed. by N. P. Cheremisinoff, Marcel Dekker, New York, Basel 1990:23–34.
- [5] Galusek D., Ghillányová K., Ceramic oxides, Ceramics science and technology. Vol. 2: Materials and properties; ed. by R. Riedel and I.-W. Chen, Wiley-VCH, Darmstadt, Ch. 2010;1:3–58.
- [6] Samanta R., Sengupta B., Mandal G., Wazeer A., Das A., Sinha A., Processing of Composites with Metallic, Ceramic, and Polymeric Matrices. [In:] Boppana S.B., Ramachandra C.G., Kumar K.P., Ramesh S. (eds), Structural Composite Materials. Composites Science and Technology. Springer, Singapore. 2024, [https://doi.org/10.1007/978-981-99-5982-2\\_5](https://doi.org/10.1007/978-981-99-5982-2_5).
- [7] Zygmuntowicz J., Wiecinska P., Miazga A., et al., Thermoanalytical studies of the ceramic-metal composites obtained by gel-centrifugal casting. *J Therm Anal Calorim* 2018;133:303–312. <https://doi.org/10.1007/s10973-017-6647-z>.
- [8] Zygmuntowicz J., Maciągowska M., Piotrkiewicz P., et al. Study of the impact of metallic components Cu, Ni, Cr, and Mo on the microstructure of  $\text{Al}_2\text{O}_3$ -Cu-Me composites. *Int J Adv Manuf Technol* 2024;133:5127–5146, <https://doi.org/10.1007/s00170-024-14070-0>.
- [9] Zygmuntowicz J., Winkler H., Wachowski M., et al., Novel Functionally Gradient Composites  $\text{Al}_2\text{O}_3$ -Cu-Mo Obtained via Centrifugal Slip Casting. *Metall Mater Trans A* 2021;52:3628–3646, <https://doi.org/10.1007/s11661-021-06334-1>.
- [10] Bednarek P., Szafran M., Sakka Y., Mizerski T., Gelcasting of alumina with a new monomer synthesized from glucose, *J Eur Ceram Soc* 2010;30(8):1795–1801, <https://doi.org/10.1016/j.jeurceramsoc.2010.01.036>.
- [11] Szafran M., Szudarska A., Bednarek P., New low-toxic water-soluble monomers for gelcasting of ceramic powders. *Adv Sci Technol* 2010;62:163–168.
- [12] Pietrzak E., Wiecinska P., Szafran M., 2-carboxyethyl acrylate as a new monomer preventing negative effect of oxygen inhibition in gelcasting of alumina, *Ceram Int* 2016;42(12):13682–13688, <https://doi.org/10.1016/j.ceramint.2016.05.166>.
- [13] Michalski J., Wejrzanowski T., Pielaszek R., Konopka K., Łojkowski W., Kurzydłowski K.J., Application of image analysis for characterization of powders. *Mater Sci Pol* 2005;23:79–86.
- [14] Wejrzanowski T., Spychalski W., Rozniatowski K., Kurzydłowski K.J., Image Based Analysis of Complex Microstructures of Engineering Materials. *Int J Appl Math Comp Sci* 2008;18:33–39, 10.2478/v10006-008-0003-1.
- [15] Wejrzanowski T., Kurzydłowski K.J., Stereology of grains in nano-crystals. *Solid State Phenomena* 2003;94:221–228, 10.4028/www.scientific.net/SSP.94.221.
- [16] Kokabi M., Babaluo A.A., Barati A., Gelation process in low-toxic gelcasting systems. *J Eur Ceram Soc* 2006;26(15):3083–3090, <https://doi.org/10.1016/j.jeurceramsoc.2005.08.020>.
- [17] Zuhair A.M., Tatsuki O., Yuji H., Mityunjay S., Innovative Processing and Manufacturing of Advanced Ceramics and Composites. Wiley 2011, 10.1002/9780470880456.
- [18] Sharifi O., Alizadeh S.M., Golmohammad M., Golestanifard F., Studying the Role of Gelation Agents in Gelcasting Non-porous  $\text{Si}_3\text{N}_4$  Bodies by Pressureless Sintering. *Silicon* 2022;14:10447–10457, <https://doi.org/10.1007/s12633-022-01798-1>.
- [19] Schmidt S.J., Thomas L.C., Thermal Analysis. In: Ismail, B.P., Nielsen, S.S. (eds), Nielsen's Food Analysis. Food Science Text Series. Springer, Cham. 2024, [https://doi.org/10.1007/978-3-031-50643-7\\_30](https://doi.org/10.1007/978-3-031-50643-7_30).
- [20] Ahluwalia V.K., Thermogravimetric Analysis. [In:] Instrumental Methods of Chemical Analysis. Springer, Cham. 2023, [https://doi.org/10.1007/978-3-031-38355-7\\_11](https://doi.org/10.1007/978-3-031-38355-7_11).
- [21] Ahluwalia V.K., Differential Thermal Analysis. [In:] Instrumental Methods of Chemical Analysis. Springer, Cham. 2023, [https://doi.org/10.1007/978-3-031-38355-7\\_12](https://doi.org/10.1007/978-3-031-38355-7_12).
- [22] Travaglini J., Barsoum M.W., Jovic V., El-Raghy T., The corrosion behavior of  $\text{Ti}_3\text{SiC}_2$  in common acids and dilute NaOH. *Corrosion Science* 2003;45:1313–1327, [https://doi.org/10.1016/S0010-938X\(02\)00227-5](https://doi.org/10.1016/S0010-938X(02)00227-5).